Fluid inclusions in emerald from the Jos complex (Central Nigeria)

Autor(en): **Vapnik, Ye. / Moroz, I.**

Objekttyp: **Article**

Zeitschrift: **Schweizerische mineralogische und petrographische Mitteilungen = Bulletin suisse de minéralogie et pétrographie**

Band (Jahr): **80 (2000)**

Heft 2

PDF erstellt am: **12.07.2024**

Persistenter Link: https://doi.org/10.5169/seals-60956

SCHWEIZ. MINERAL. PETROGR. MITT. 80, 117–129, 2000

Fluid inclusions in emerald from the Jos complex (Central Nigeria)

by *Ye. Vapnik*[1] and *I. Moroz*[2]

Abstract

Fluid inclusions in emerald from the Jos complex, Central Nigeria, were investigated by microthermometric and Raman techniques. The emerald was sampled in a miarolitic cavity of alkaline granite affected by autometasomatic albitization. Primary fluid inclusions are randomly distributed within the central part of the emerald and arranged along the growth faces of crystals in the middle and outer parts of the emerald. Pseudosecondary inclusions are present in every emerald growth stages. There are two types of fluid inclusions: (1) multiphase inclusions which are composed of a Na–Ca–Cl solution with a bulk salinity up to 45 wt%, low-density volatile phase ($CO_2 \pm CH_4 \pm H_2S$), halite and calcite ± Mg-calcite ± aragonite; (2) volatile-rich, water-free and water-bearing CO_2 fluid inclusions with a CO_2 phase of very low density (< 0.13 g/cm^3). Both types of inclusions are distributed within the middle and outer parts of the emerald and related to the emerald growth. Fluid inclusion data indicate emerald crystallization conditions of the early and intermediate growth stages at 400 to 450 °C and 0.2 to 0.3 kbar.

Keywords: Nigeria, emerald, fluid inclusions, microthermometry, Raman spectroscopy, PT trapping conditions.

Introduction

Most of the emerald occurrences in Australia, Brazil, Mozambique, Russia, Tanzania (Lake Manyara), Zambia etc. are associated with granites and pegmatites. They are located in regions where acidic magmas have penetrated country rocks in the vicinity of Cr-bearing basic-ultrabasic rocks (BEUS and MINEYEV, 1974; KIYEVLENKO et al., 1974; MOROZ, 1978; GRAZIANI et al., 1983; BROWN et al., 1984; SLIWA and NGULUWE, 1984; SINKANKAS and READ, 1986; SCHWARZ, 1987; KAZMI and SNEE, 1989; RUDOWSKI, 1989; SCHWARZ and EIDT, 1989; SCHWARZ, 1991; LAURS et al., 1996; MOROZ, 1996; GIULIANI et al., 1997, 1998; MOROZ and ELIEZRI, 1998a). The circulation of hydrothermal fluids channeled by pegmatites resulted in plagioclasite formation at the expense of pegmatites and biotite-phlogopite rock formation at the expense of chromite-bearing basic-ultrabasic rocks (GIULIANI et al., 1997; 1998).

Emerald is hosted either by phlogopite-bearing rocks or by plagioclasites. The geochemistry of the emeralds from these deposits is characterized by high MgO (0.7–3.1 wt%), FeO (0.3–1.8 wt%) and Na_2O (0.2–2.8 wt%) concentrations and features an unusual quantitative and qualitative combination of elements of, on the one hand, acidic magmas (e.g. beryllium, sodium, potassium, zinc and cesium), and, on the other hand, ultrabasic or basic country rocks (e.g. magnesium, iron, chromium, vanadium, titanium, nickel, cobalt and copper) (MOROZ and ELIEZRI, 1998a). This emphasizes the metasomatic hydrothermal nature of these emeralds.

Ore consists usually of phlogopite rock bodies that are related to metasomatic associations in mafic-ultramafic country rock containing variable quantities of talc, tremolite, chlorite, etc. (MOROZ, 1978; 1979; 1983; 1996). Some of these minerals formed as solid inclusions during the emerald growth (SCHWARZ, 1987; MOROZ and ELIEZRI,

[1] Department of Geological and Environmental Sciences, Ben-Gurion University of the Negev, P.O.B. 653, Beer-Sheva 84105, Israel. <vapnik@bgumail.bgu.ac.il>

[2] The Institute of Earth Sciences, The Hebrew University of Jerusalem, Giv'at Ram, Jerusalem 91904, Israel. <inessa@vms.huji.ac.il>

1998b; 1999) and were also found within the emeralds studied in the present paper.

A genetic model for the Nigerian gemstones, that are associated with Mesozoic alkali granite ring complexes subjected to autometasomatic alteration, has been proposed by SCHWARZ et al. (1996). The Nigerian gems are a particular type of pegmatite-related deposits (GIULIANI et al., 1997) formed by the alkaline alteration of granites.

The genesis of emerald, P-T conditions of emerald formation, composition of fluid responsible for emerald growth are the questions often risen by gemmologists. Study of fluid inclusions in emerald is a mean to answer these questions (GRUNDMANN and MORTEANI, 1989; KAZMI and SNEE, 1989; SOUZA et al., 1992; NWE and MORTEANI, 1993; CHEILLETZ et al., 1994; GIULIANI et al., 1995; MOROZ and VAPNIK, 1998; 1999).

Up to now, a few preliminary data on fluid inclusions hosted in emeralds of Central Nigeria and some conclusions on their trapping conditions were performed (KINNAIRD, 1985; SCHWARZ et al., 1996). One of the conclusions of these studies was that fluid inclusions in Nigerian emeralds showed an inclusion pattern similar to that of Colombian emeralds (SCHWARZ et al., 1996). The comparison concerns the fluid inclusions only as far as the Nigerian and Colombian emeralds belong to different types of emerald hosted deposits (GIULIANI et al., 1997). The Colombian deposits are unique because they are hosted within black shale series. Emerald formation was due to decollement planes, thrusting and thrust-fault related folds promoting hydrothermal fluid infiltration and a strong fluid-rock interaction with the black shales (CHEILLETZ and GIULIANI, 1996).

Our data on fluid inclusions in the Nigerian emerald and their comparison with the published data on Colombian emeralds permit to reason that although the petrography of fluid inclusions can be similar, they may show many different features during freezing-heating experiments. So, we believe that the distinction between the Colombian and Nigerian emeralds can be also made by the data on fluid inclusions.

Geological setting

The oldest rocks of the Nigerian Basement Complex were originally sediments and granite bodies which have undergone folding and metamorphism and have been metamorphosed to migmatites and granite gneiss. Younger sediments were deposited onto the basement and were folded together with this granitized basement during the Pan-African orogeny (from 750 to 450 Ma). Linearly oriented schist belts of low-grade metasedimentary rocks were formed. Granitoids associated with the Pan-African orogeny were intruded into both the Basement Complex and the younger metasedimentary cover. The closing stages of the orogeny were marked by cooling, uplift and fracturing, by the eruption of volcanic rocks and the formation of pegmatitic lenses and dykes (SCHWARZ et al., 1996).

The younger granites emplaced during the period 190 to 144 Ma, form ring complexes typically 2–25 km in diameter. The granitoid suite consists of more than 95% granite, while intermediate and basic rocks constitute less than 5% of the area. There are several distinctive granite types: (a) peralkaline granite and related syenites with alkali or calcic amphibole; (b) peralkaline biotite alkali feldspar granites and biotite syenogranites; (c) metaluminous fayalite and hornblende-bearing granites and porphyries with amphiboles and biotite (KINNAIRD, 1979; 1985). Ring complexes are the products of mantle-derived magmas that have undergone a strong crustal contamination during their ascent and differentiation in the crustal basement (DICKIN et al., 1991).

In the alkaline granites a series of hydrothermal alteration processes with related mineralization resulted from differing degrees of interaction of escaping fluids on originally magmatic rocks have been recognized (BOWDEN, 1982). The gem varieties of beryl are associated with early sodic metasomatism (albitization). The emeralds occur in two settings both formed under similar geological conditions: (1) in small pegmatitic pockets in association with quartz, feldspar and topaz. The pegmatite pockets, which are up to 8 cm in size, are found at the contact of a granite with country rocks and represent cavities created by gas loss from the cooling magma; (2) in small miarolitic cavities which formed by gas loss in the "roof" of granite within a zone of < 20 m from its upper contact with the overlying rocks of the Basement Complex (SCHWARZ et al., 1996).

The source of Cr in the Nigerian beryls is problematic. However, most emerald formation occurs close to the "roof" of a granite in the region where granite fluids may have interacted with surrounding country rocks. It is likely that Cr may has been incorporated from the basement schists or younger volcanic rocks both of which have higher Cr-contents than granites (SCHWARZ et al., 1996).

Sample description

The studied emeralds belong to the Jos granitoid ring complexes. The emeralds were found in small miarolitic cavities and were provided by Israel's Emerald Cutters Association. The three available emerald crystals, ranging from 8 × 4 × 3 mm to 10 × 6 × 6 mm in size, represent the full range of color-tone and saturation, as well as hue between bluish-green and yellowish-green. The rough crystals are predominantly euhedral prismatic. Fluid inclusions were rather rarely distributed in two emerald samples whereas the third biggest crystal was richest in fluid inclusions. It was selected for detailed study presented here. The crystal had eye-visible color zoning and additional colorless zone (the center of the crystal), typically noted parallel to the prism faces. The diaphaneity of the crystal ranged from transparent to translucent, depending on the nature and number of inclusions present. Weak-to-prominent growth structures were seen in the sample examined. Most common were strongly developed straight and angular sequences of prism, basal-pinacoid and pyramid planes, which were consistent with the descriptions given by SCHWARZ et al. (1996).

The Nigerian emerald is characterized by low magnesium (0.00–0.08 wt%) and sodium (0.00–0.67 wt%) contents; FeO content is in the range of 0.1–0.73 wt%. The analyses revealed up to 0.19 wt% of Cr_2O_3 (Tab. 1). The oxides of other elements such as V_2O_3, CaO, K_2O, TiO_2, MnO, Cs_2O and CuO were found in amounts near the detection limit of the electron microprobe used. The emerald was remarkable for its considerable content (up to 0.49 wt%) of SO_3 (MOROZ and ELIEZRI, 1998a). The Nigerian and Colombian emeralds show geochemical similarity, but the first has higher iron and lower magnesium contents (Tab. 1). Compared with emeralds from other deposits, the Nigerian and Colombian emeralds show the lowest Na_2O values (MOROZ and ELIEZRI, 1998a). The incorporation of Na in the channels of the emerald structure does not depend on its availability in the mineralizing fluid. The controlling factor is the need for charge compensation caused by the entrance of bivalent cations. Consequently, the Na-concentration is low because ($Mg+Fe^{2+}$) in the emeralds is also low (SCHWARZ et al., 1996).

Tab. 1 Chemical composition (wt%) of the Colombian and Nigerian emeralds.

Location	Colombia	Nigeria
Deposit	Muzo	Jos
No. of samples	2	3
No. of analyses	14	17
Cr_2O_3	<–0.29	<–0.19
V_2O_3	<–0.21	<–0.16
FeO	<–0.25	0.09–0.73
MgO	<–0.76	<–0.08
Na_2O	<–0.65	0.10–0.67
Cs_2O	<–0.23	<–0.19
SiO_2	62.2–66.5	63.4–67.2
Al_2O_3	16.8–18.0	17.8–19.2
MnO	<–0.12	<–0.11
TiO_2	<–0.17	<–0.12
CaO	<–0.23	<–0.18
K_2O	<–0.03	<–0.10
SO_3		<–0.49
CuO	<–0.41	<–0.21
NiO		<–0.22
ZnO	<–0.25	

<–: Concentration of element below detection limit of microprobe.

One peculiarity of the Nigerian deposits is related to a set of solid mineral inclusions trapped by emerald during its growth. The following mineral inclusions were found: chlorine-bearing Al-glauconite, copper-antimony sulfide, tourmaline, Fe-oxide, fluorite, albite, quartz, beryl and euclase (MOROZ and ELIEZRI, 1998b; 1999).

Al-glauconite is likely formed by the alteration of biotite. The Mg/Fe ratio in illite-glauconite-celadonite inclusions in emeralds from most deposits is in the range of 2.2–7.2; the reverse ratio of these elements of about 0.5 is characteristic for Al-glauconite inclusions in the Nigerian emeralds (MOROZ and ELIEZRI, 1998b). Mg/Fe ratio in illite-glauconite-celadonite inclusions in emeralds correlates with concentration of these elements in emeralds and reflects a country rock composition (MOROZ and ELIEZRI, 1998a). Several substitutions of Cr, Ti and Zn are recorded for the octahedral site and Cl and S for the hydroxyl site of Al-glauconite. The crystallochemical formula of the mineral obtained by various microprobe analyses is as follows:

$$(K_{0.42}Na_{0.12}Ca_{0.065}Cs_{0.002})_{0.61}(Al_{1.17}Fe_{0.64}Mg_{0.31}Ti_{0.054}Zn_{0.02}Cr_{0.005})_{2.20}[(Si_{3.5}Al_{0.5})_4O_{10}][OH,Cl,S_{0.05}]_2 \cdot nH_2O$$

Analytical techniques

Several chips cut perpendicular to the c-axis of the emerald were investigated. From these chips 0.2–0.1 mm thick emerald wafers polished on both sides were prepared. Microscopic examination of the emerald wafers revealed several populations of fluid inclusions.

Fluid inclusions were studied at temperatures between –190 and +500 °C with a Fluid INC. heating-freezing stage. The accuracy of temperature measurements is about ± 0.5 °C in the low-

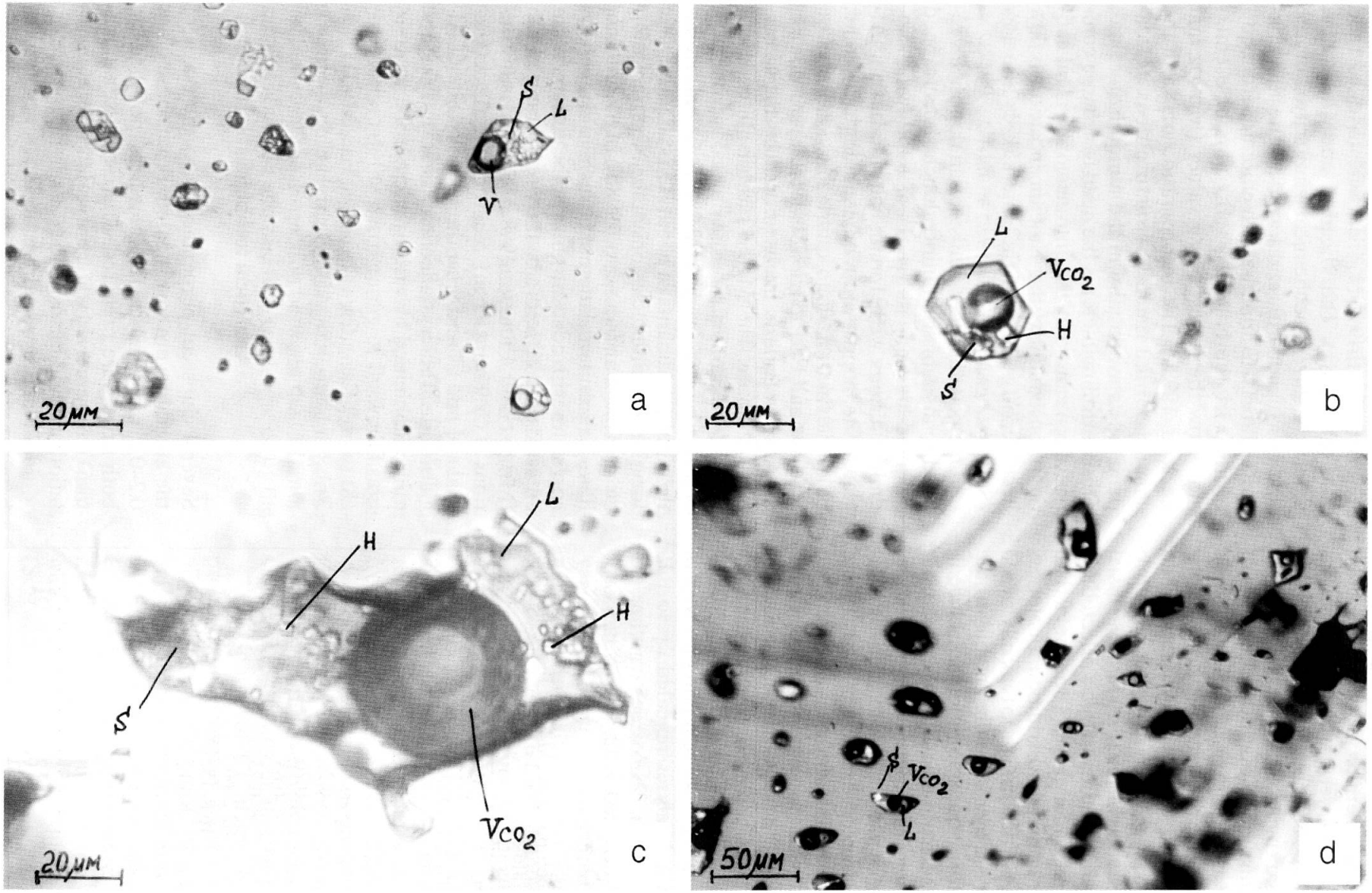

Fig. 1 Fluid inclusions in the Nigerian emerald. Liquid (L), vapor (V), halite (H) and birefringent solid (S) phases are shown.
(a) Multiphase primary inclusions in the central part of the emerald. (b) Multiphase primary inclusions in the central part of the emerald. (c) Multiphase pseudosecondary inclusion in the central part of the emerald. Crossed nicols. The numerous small halite cubes which were formed after the freezing and following heating up to ambient temperature, are clearly discernible in the inclusion. (d) Multiphase primary inclusions along the growth faces of the emerald (the middle part of the emerald). Crossed nicols.

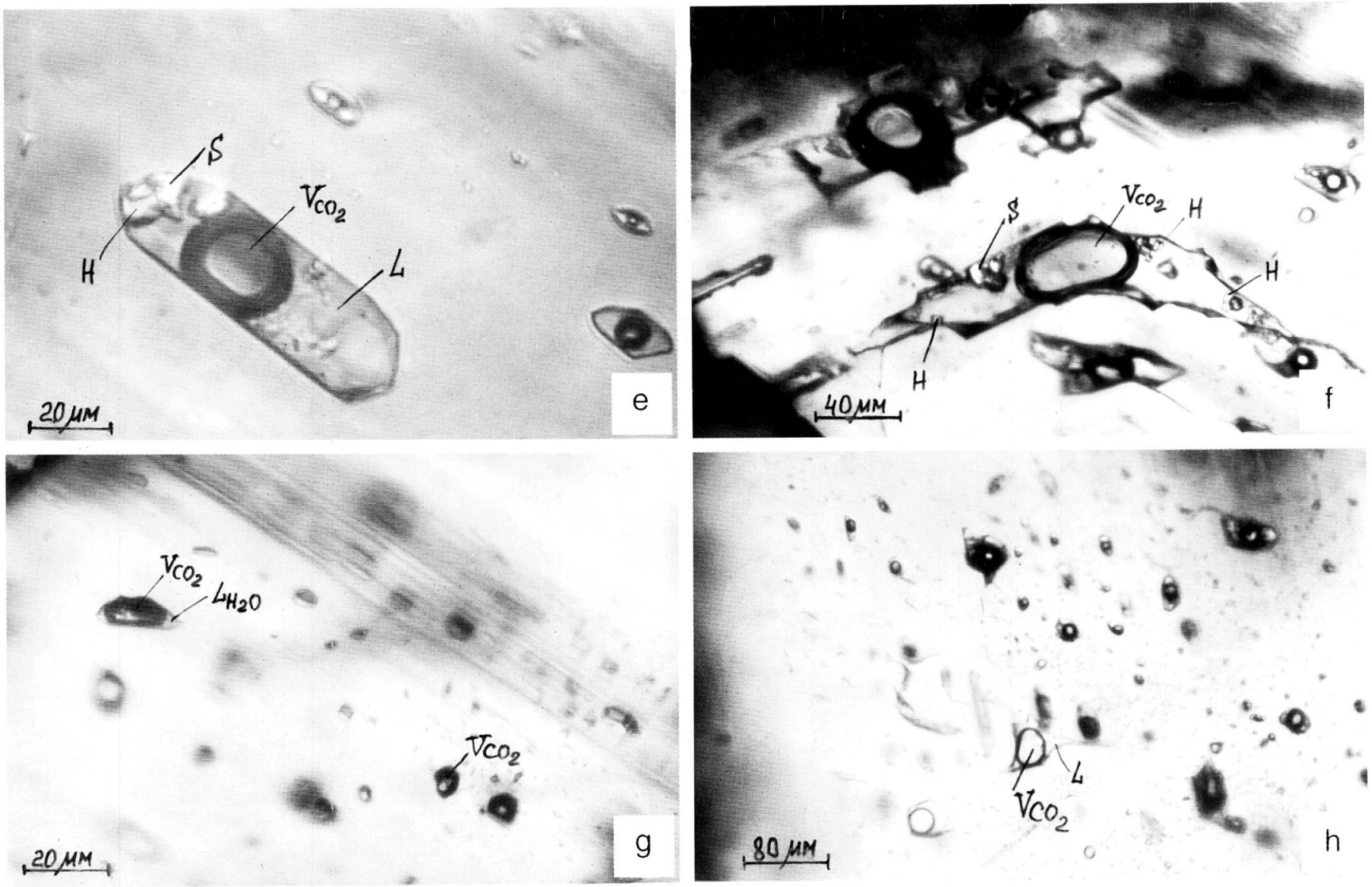

Fig. 1 (cont.) (e) Multiphase primary inclusion in the middle part of the emerald. Crossed nicols. (f) Multiphase primary inclusion at the jointing of crystal faces (the outer part of the emerald). Crossed nicols. (g) Volatile-rich CO_2-bearing primary inclusions along the growth faces of the emerald (the middle part of the emerald). (h) The latest primary and pseudosecondary inclusions in the outer part of the emerald. The rim of the crystal is seen to the left.

temperature range (–190 to + 50 °C) and ± 5 °C in the high temperature range (100–500 °C). The temperature data on phase transitions in brine inclusions were obtained by the method of sequential heating and freezing (HAYNES, 1985; ZWART and TOURET, 1994).

The analysis of solid and gaseous phases in fluid inclusions was performed using an Ar+ Raman microspectrometer (Renishaw system, 1000, Institute of Earth Sciences, Jerusalem). The green polarized light of an Ar+ laser beam was used for excitation. Raman spectrum was collected by × 50 objective of the Leica optical microscope. The emitted light is dispersed and analyzed through a spectrometer equipped with a CCD detector. Using entrance slits of 100 μm, the spectral line width is about 3.5 cm^{-1}, with a resolution of less than 1 cm^{-1} and a frequency reproducibility of the same order. The spectrum acquisition time was 100 sec. A standard PC computer was used to collect and store Raman spectra, as well as allowing data analysis and presentation. The presence of the volatile components CO_2, CH_4, N_2, and H_2S was checked referring to the following lines, respectively: 1388 cm^{-1}; 2917 cm^{-1}; 2331 cm^{-1}; 2611 cm^{-1} (BURKE, 1994).

Petrography of fluid inclusions

Primary inclusions are formed during crystal growth (ROEDDER, 1984). In the Nigerian emerald primary inclusions represented by clusters of randomly distributed inclusions were found in the central, colorless part of emerald (in a distance of about 0–1 mm from the center to rim of the emerald). Primary inclusions were also distributed along growth faces in the middle and outer parts of the crystal studied.

Pseudosecondary inclusions are formed during or toward the end of crystal growth. Rare trails of pseudosecondary inclusions were found along the healed small fractures. A few trails of latest inclusions originated at the crystal boundary (secondary or latest pseudosecondary inclusions) were also found. As a rule, inclusions within the healed fractures are oriented along the growth faces of the emerald.

The central part of the emerald is filled by a cluster of small multiphase inclusions (primary inclusions, Fig. 1 a and b). Some of the multiphase inclusions arrange along small linear trails (pseudosecondary inclusions). The size of inclusions is usually up to 10 μm, and only a few of them are up to 20 μm. They are composed of a gas bubble

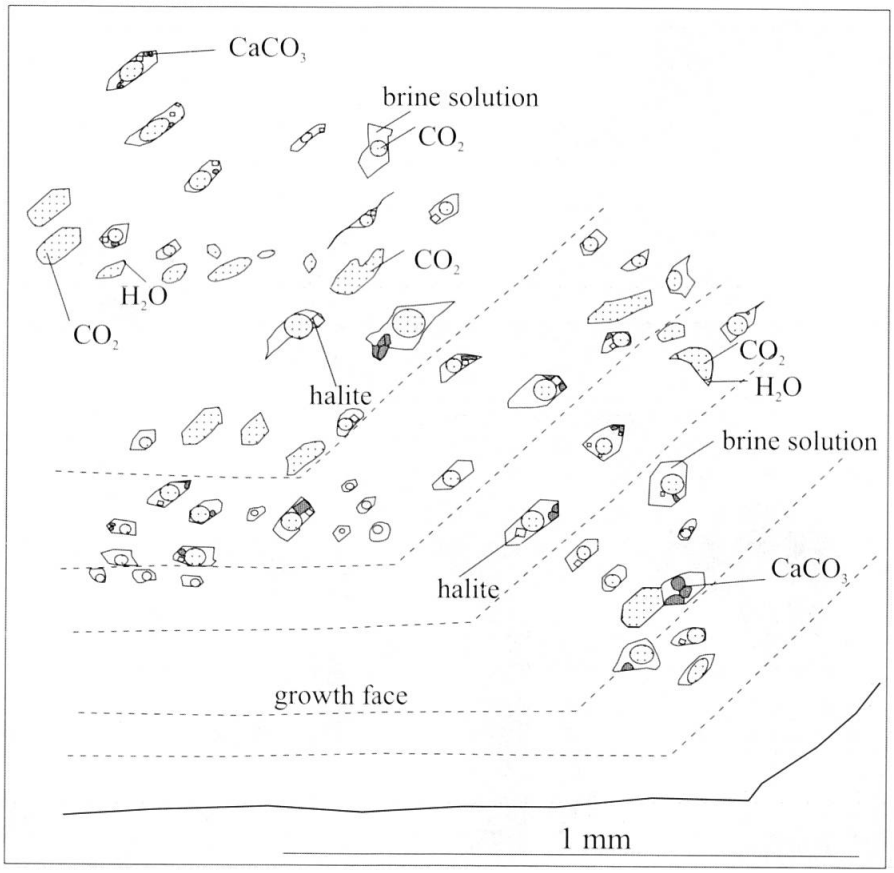

Fig. 2 Sketch of typical distribution of multiphase and volatile-rich inclusions in the emerald.

(about 20–30 vol%), a liquid (about 30–50 vol%), one or several halite crystals (about 10–20 vol%), and birefringent phases are also often present.

Inclusions related to the growth zones of emerald are abundant in the middle and outer boundary of the emerald (primary inclusions, Figs 1d, e and f; Fig. 2). Inclusions are generally of about 30–40 μm, but some of them are up to 100–200 μm. Large inclusions sometimes follow the jointing of crystal faces, forming curve-shaped inclusions (Fig. 1f). Sometimes necking down phenomenon is evident. Most of the large inclusions are formed at the outer boundary of the emerald. Inclusions are multiphase and composed of a liquid (about 50–70 vol%), gas bubble (about 20–40 vol%), one or several small rounded birefringent and/or isotropic phases and isotropic phase represented by halite (about a few vol%).

Volatile-rich inclusions (the gas is about 70 up to 100 vol%) are related to the growth zones of the emerald (primary inclusions, Figs 1g, 2) or to the linear trails (pseudosecondary inclusions). In the last case inclusions are also oriented along the direction of crystal face growth. The volatile-rich inclusions were observed on one or two faces of crystal in the middle and outer parts of emerald. The inclusion size is up to 40 μm, small isotropic and/or birefringent phases may sometimes be seen in the liquid part of inclusions.

Latest pseudosecondary inclusions related to the outer boundary of emerald may have different liquid/gas ratio (0–50 vol% of gas). A lot of necking down is characteristic here and homogeneous trapped fluid inclusions superimposed by fluid inclusions showing younger necking down phenomenon (Fig. 1h). Halite and one or two small solid phases are usually present in these inclusions.

Results

MULTIPHASE INCLUSIONS

Lowest-temperature phase changes were observed in the biggest inclusions only. Tiny rounded solid phases that formed during the freezing in the gas bubbles melted and/or recrystallized in the range of –122 to –56.6 °C. Other phase changes in biggest and smaller inclusions during cyclic heating and freezing experiments are very complicated. They are likely due to the composite nature of solution, crystallization and melting of clathrate, general metastability of inclusions themselves and often metastability of phases crystallized during the cooling. The general metastability of inclusions may be illustrated by the appearance and the stability at ambient temperature of numerous small halite cubes (sometimes about 20–30 small crystals, Figs 1c and f) which were absent in inclusions before the start of the cooling experiments. The appearance of many new small halite cubes, reaction halite-hydrohalite, low-temperature clathrate melting make impossible unambiguous measurements of some melting temperatures.

In general, the initial ice melting was observed at a temperature range of –63.0 to –40.0 °C (Fig. 3a). The last melting of ice (Tm_i) was generally at temperatures of –27.0 to –18.0 °C (Fig. 3a). Hydrohalite started melting at –55.0 to –15.0 °C, the final melting of hydrohalite took place at –10.0 to +15 °C (Fig. 3b). The hydrohalite-halite transformation reaction was clearly observed in most inclusions at positive temperatures. The final melting of fibrous solid around vapor bubble was observed in the range of –34.0 to –22.0 °C (clathrate melting, Fig. 3a). The dissolution of halite (Tm) was observed at 50–220 °C (Fig. 4a). The disappearance of vapor (Th) was observed at 250–520 °C (Fig. 4a). Small isotropic and birefringent phases were in most cases insoluble during the heating, but in some inclusions their dissolution was observed between 400– 470 °C (Fig. 4a). A lot of decrepitation usually started at > 450 °C.

The dissolution temperature of halite in the fluid inclusions are of the same range in the central (0–1 mm from the crystal center), middle (1–2 mm) and outer (2–3 mm) emerald growing zones. The data on the Th of fluid inclusions in the central, middle and outer emerald growing zones are shown in Fig. 4b. There is a weak tendency of Th to decrease from the center to the outer emerald growing zones.

Solid daughter phases were investigated in about 20 fluid inclusions by Raman analysis. Only in 6 fluid inclusions birefringent solid phases were Raman active and revealed prominent Raman shifts of peaks at 1085 cm^{-1}, 1087 cm^{-1}, 1088 cm^{-1} and 1089 cm^{-1} (Fig. 5b). These daughter minerals were identified as calcite (in three cases), Mg-calcite (in four cases) and aragonite (in one case) (BURKE, 1994).

The gaseous phase in a few inclusions where low-temperature melting or recrystallization had been observed during cooling-heating experiments was also studied by Raman analysis. Very minor intensity shifts were observed at 1388 cm^{-1} only, indicating low-density CO_2.

VOLATILE-RICH INCLUSIONS

These inclusions are mainly composed of a very low-density gas phase with a water phase which is

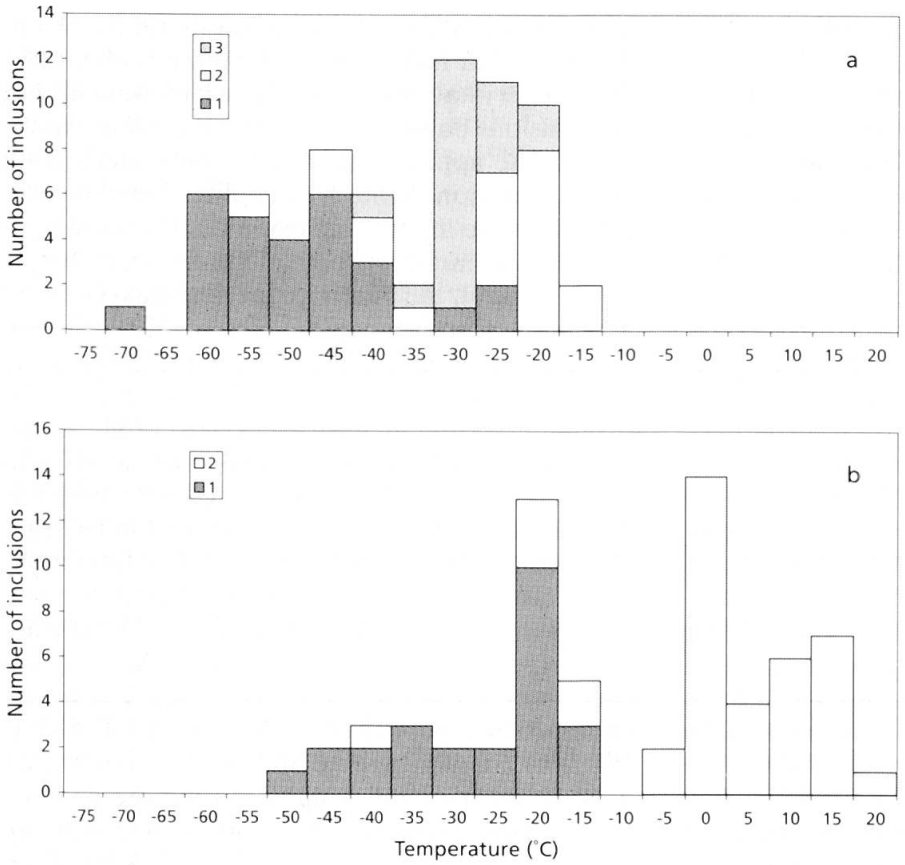

Fig. 3 Histograms showing the low-temperature data on multiphase inclusions.
(a) 1. Initial ice melting (eutectic temperature); 2. Final temperature of ice melting (Tm_i); 3. Final temperature of clathrate melting.
(b) 1. Initial hydrohalite melting; 2. Final temperature of hydrohalite melting.

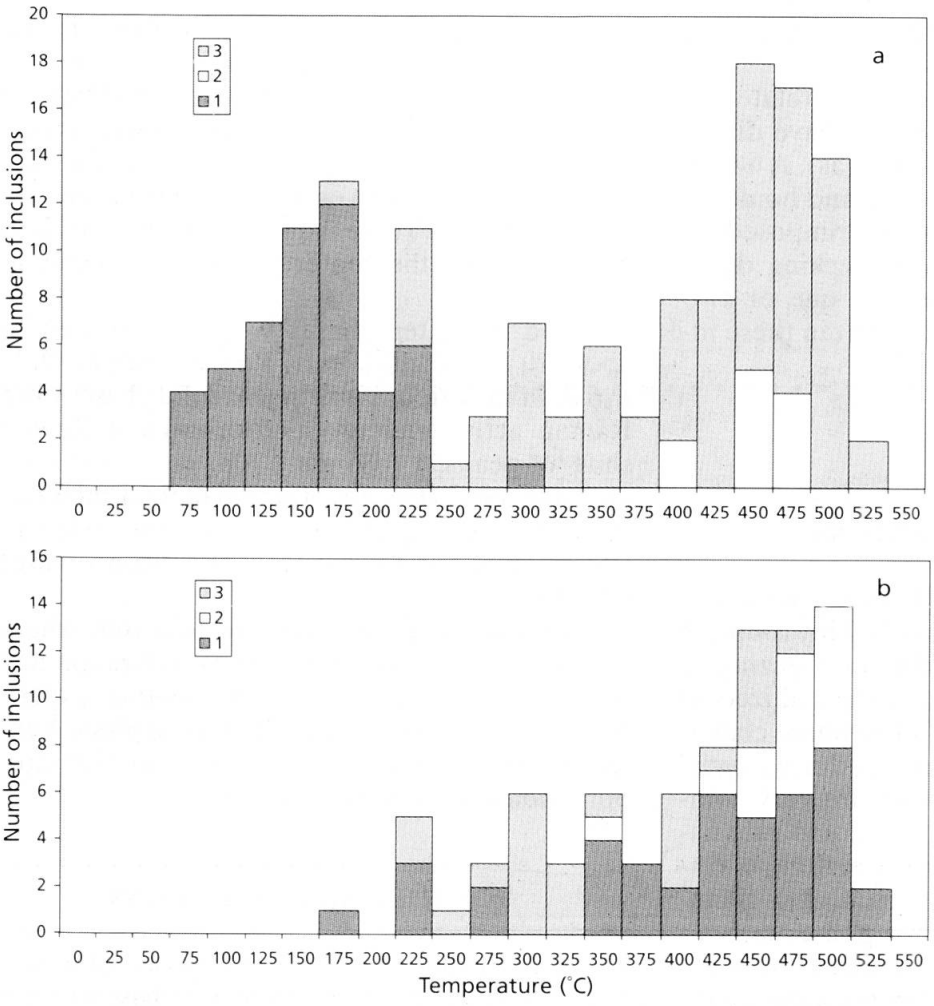

Fig. 4 Histograms showing the high-temperature data on multiphase inclusions.
(a) 1. Halite dissolution temperature; 2. Dissolution temperature of small isotropic and/or birefringent phases; 3. Temperature of homogenization (Th L + G -> L).
(b) Temperature of homogenization (Th L + G -> L) in the central (1), middle (2) and outer (3) emerald growing zones.

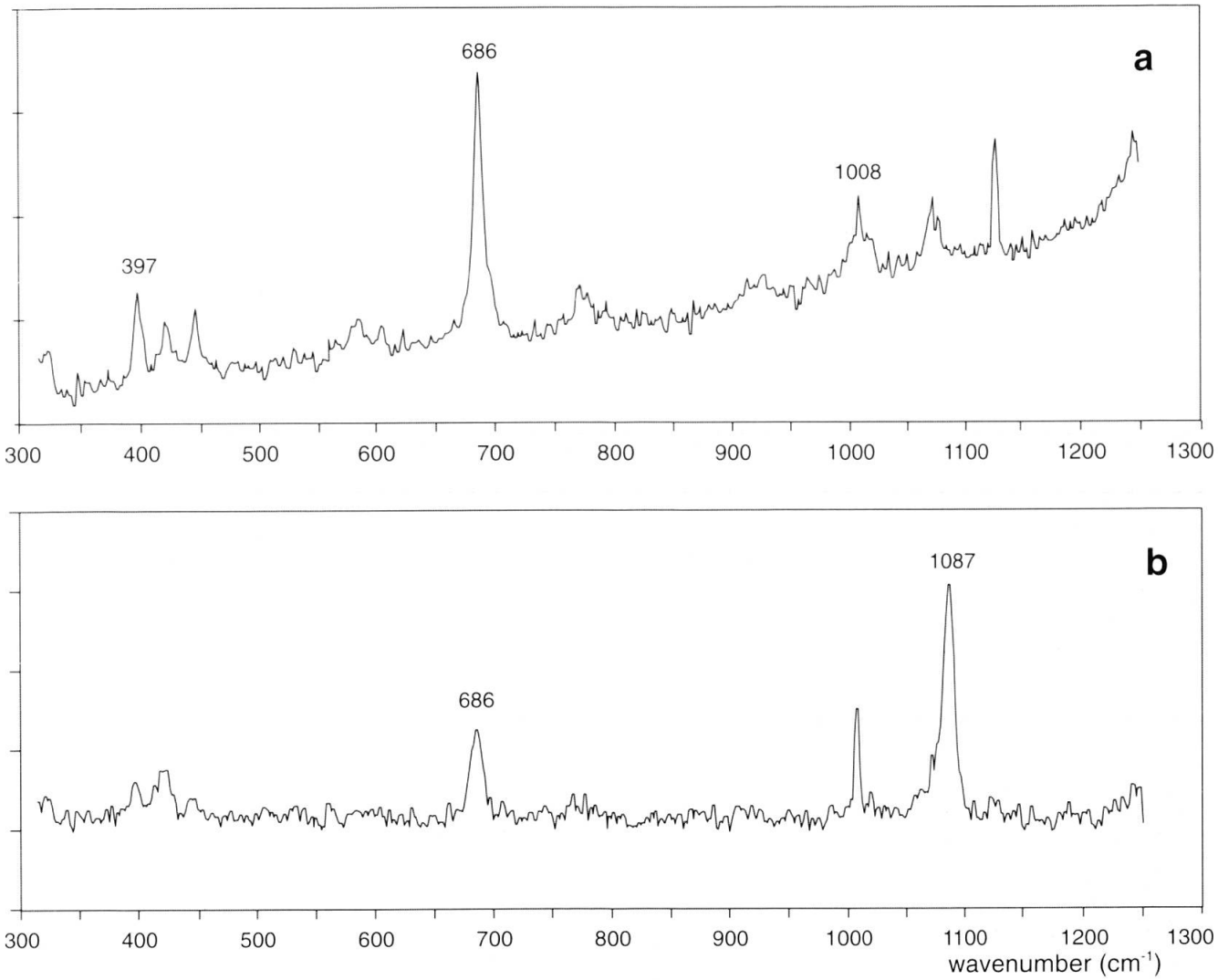

Fig. 5 Raman spectrum of emerald (a) and emerald + Mg-calcite (b).

usually under the microscope detection limit (water content is usually lower than 20 vol%). So, only a few microthermometric data could be obtained during heating-freezing runs. The melting of solid phases in the gas bubble were observed in a few inclusions at –56.6 °C indicating pure CO_2. The temperature of CO_2 homogenization (Th CO_2) was observed at –45.0, –10.0, 2.5, 5.0 and 11.0 °C into the gas phase, indicating a very low density of CO_2. The complete homogenization temperature for a few gas-liquid inclusions is 170, 250 and 290 °C into the gas phase. Tiny isotropic or birefringent solid phases may be sometimes seen in volatile-rich inclusions. No dissolution of these solids was marked during the heating.

Discussion

Complexes of Be^{2+} with fluoride, hydroxide, carbonate and chloride have been proposed for the transport of Be under low- to high-temperature conditions (e.g. GOVOROV and STUNZHAS, 1963; BEUS and DIKOV, 1967; BROWN et al., 1983; WOOD, 1992). The anions in the fluids percolated in the Jos deposit were dominated by F and Cl, as determined from fluoride (fluorite, boldyrevite and ralstonite), fluorosilicate (SCHWARZ et al., 1996) and chloride inclusions in the emerald. Boron was also in the solution (tourmaline inclusions). Be-fluoride complexes become unstable when a_{F^-} decreases, which may be caused by precipitation of fluorides (WOOD, 1992). At the Jos deposit, fluoride precipitation is expected to cause beryl precipitation from fluoride complexes causing the residual fluid enrichment in Cl. This residual fluid was trapped by the growing emerald in fluid inclusions.

Multiphase primary and pseudosecondary inclusions are the most abundant type of fluid inclusions in the emerald. They have different size and appearance (they can be with or without isotropic and/or birefringent phases), in spite of that they show rather similar gas/liquid ratio and behave similarly during heating-freezing experiments. The general metastability of inclusions is evident

and reflected in the appearance of halite small crystals during cooling and then halite stability sometimes up to 190 °C. In general, the low-temperature behavior of inclusions is similar to Ca–Na–Cl inclusions described by ZWART and TOURET (1994). Using the data on Tm_i of ice (–27.0 to –18.0 °C), Tm of hydrohalite (–10 to 15 °C), and Tm of halite (50 to 220 °C) it is possible to roughly evaluate the composition of inclusions.

It is as follows: $NaCl/CaCl_2/H_2O$ = 30/10/60 (VANKO et al., 1988). The dissolution of halite at 50–220 °C indicates a NaCl concentration of up to 33 wt% (ROEDDER, 1984). Thus, the whole salinity of solutions is about 40–45 wt%. The high NaCl content in the fluid phase participating in the emerald growth is confirmed by albite and Cl-bearing glauconite syngenetic inclusions in the emerald. High calcium content in fluid is supported by $CaCO_3$ daughter phases often identified by Raman analysis in multiphase inclusions and by fluorite syngenetic inclusions in the emerald.

The low-temperature phenomenon of clathrate melting is similar to oversaturated brine-CO_2–CH_4–H_2S inclusions described by ZWART and TOURET (1994). So, based on the referenced low-temperature clathrate melting (ZWART and TOURET, 1994) the CH_4–CO_2–H_2S composition of a very low dense volatile phase at very low fluid pressure was suggested. Relatively high content of H_2S in gaseous phase is confirmed by increased SO_3 content in the emerald, copper-antimony sulfide and S-bearing glauconite syngenetic inclusions in the emerald (MOROZ and ELIEZRI, 1999). It is likely that due to the very low-density of the gaseous phase it was impossible to detect the admixtures of CH_4 and H_2S to CO_2 by Raman analysis. Considering the very low density of vapor phase, the gas content of inclusions is about a few percents.

The temperature of multiphase inclusion homogenization (Th) is in the range of 200–520 °C. Most inclusions are homogenized between 400–500 °C (Fig. 4a) and mainly at about 450 °C. Due to the usual decrepitation of inclusions at about 450 °C the measured higher temperatures of homogenization correspond to stretched or partly decrepitated inclusions. This is indicated at room temperature comparing gas/liquid ratio, that becomes larger after heating than before. Thus, partial reequilibration (e.g. VITYK and BODNAR, 1998), partial decrepitation, and partial necking down leading to slightly different composition of fluid inclusions are likely responsible for different Th within the same population of fluid inclusions. The statistical approach to the Th data indicates a minimum temperature of inclusion trapping of about 400–450 °C.

Primary and pseudosecondary volatile-rich inclusions are mainly composed of low-density CO_2 and a water phase at quantities of about its detection limit under the microscope (about ≤ 20 vol%). The volatile-rich inclusions were found among the multiphase inclusions along linear trails or along the emerald growing faces in the middle and outer parts of the crystal on some (one or two) faces of the emerald (Fig. 2). The distribution character of multiphase and volatile-rich inclusions suggests their contemporaneous trapping. Very low density of CO_2 in the gaseous inclusions and respectively the low trapping pressure of gaseous inclusion put in question the possibility of gaseous and multiphase inclusion trapping due to fluid heterogenization. Thus, an inflow of low-density CO_2-rich fluid at the middle and outer stages of the emerald growth has to be assumed. The contemporaneous trapping of volatile-rich and multiphase inclusions permits to use the data on them for the estimation of temperature and pressure during inclusion trapping (Fig. 6). The Th of multiphase inclusions indicates the likely temperature of inclusion trapping of 400–450 °C, whereas the phase diagram of the $NaCl$–H_2O system outlines the lowest possible range of trapping pressure. The absence of gaseous water-rich inclusions of low salinity coexisting with liquid salt-rich inclusions in the emerald and homogeneous trapping of salt-rich inclusions indicate that salt-rich inclusions have been trapped in the field of single-phase fluid. At the temperature range of 400–500 °C and fluid bulk salinity of about 40 wt% a single phase fluid is stable at P > 0.15–0.5 kbar (BODNAR and VITYK, 1994). Using the data on volatile-rich inclusions (CO_2 density, CO_2/H_2O volume ratios) and trapping temperature of multiphase inclusions the following trapping pressure of volatile-rich inclusions can be estimated: P ≈ 0.2–0.3 kbar (extrapolation of the data of BROWN and LAMB (1989) to the low-density field of CO_2).

Collected data on fluid inclusions in the Nigerian emerald permit to compare them with the data on the Colombian emerald (GIULIANI et al., 1992, 1993; CHEILLETZ et al., 1994). Both emeralds formed from essentially Na–Ca–Cl-rich solutions. Halite is a common phase in fluid inclusions, and inclusions show a similar range of the eutectic and Tm_i melting temperatures. CO_2 is usually present in the gaseous phase. In the studied emerald liquid CO_2 is not visible at room temperature, but the presence of three-phase CO_2-bearing fluid inclusions has been found in the Nigerian emeralds (GIARD et al., 1998). Liquid and vapor CO_2 are also typical for the Colombian emeralds. H_2S was suggested in the vapor phase of the fluid inclu-

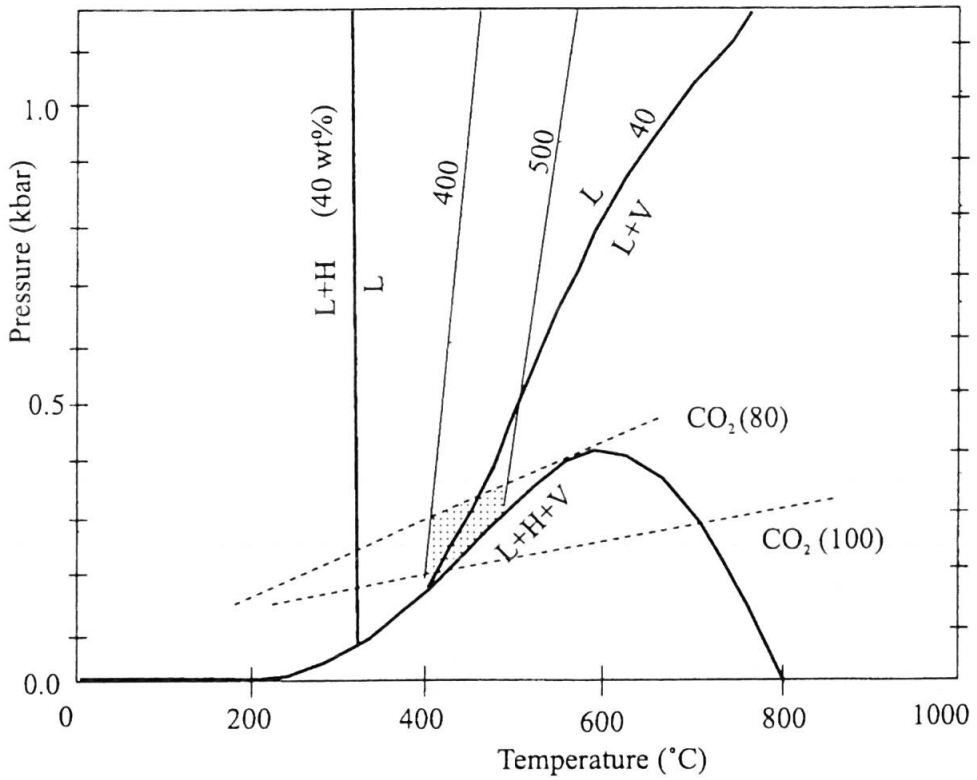

Fig. 6 PT-conditions during the emerald growth. The bold solid lines correspond to a P-T plot of a part of the system NaCl–H_2O. H – halite, L – liquid, V – vapor. L + H + V three phase curve; L + H > L (40 wt%) – the liquidus curve for 40 wt% NaCl (the total salinity NaCl + $CaCl_2$ was referred to the bulk density as NaCl equivalent); L > L + V vapor-pressure curve for H_2O–NaCl solution with salinity 40 wt%. Solid lines are isochores originating at 400 and 500 °C, respectively, for inclusions having salinity of 40 wt% NaCl (BODNAR and VITYK, 1994). Dashed lines are isochores of the low-density CO_2 system. CO_2 (100) – pure CO_2 (SHMULOVICH et al., 1982); CO_2 (80) – isochore of 80 vol% CO_2 and 20 vol% H_2O (BROWN and LAMB, 1989). Hatched area is the PT-field of isochore intersections.

sions of the Nigerian emerald. SO_4 was also found in the inclusions of the Colombian emerald (BANKS et al., 1995).

It is likely that the following descriptive characteristics of fluid inclusions in the Nigerian emerald may be used for the determination of an emerald source:

(1) low temperature of clathrate melting which is likely indicative for H_2S (ZWART and TOURET, 1994) present in the gaseous phase of inclusions;

(2) the common metastability of fluid inclusions. Many inclusions are without a cubic crystal of halite, but numerous crystals of halite usually appear after inclusion is frozen and re-melted again. The metastability was also reported for fluid inclusions in Colombian emeralds, where hydrates were nucleated during the cooling and stable in the range of 50–284 °C (GIULIANI et al., 1993);

(3) the existence of volatile-rich inclusions (low density CO_2 +/– H_2O inclusions) on one or two faces of emerald;

(4) the different character of inclusion homogenization. Nigerian emeralds show the dissolution of halite and then the dissolution of the gas phase (the Colombian scheme of homogenization is reverse), which is directly connected with higher temperatures of the Nigerian emerald genesis.

The obtained data on fluid inclusions in the Nigerian emerald constrain the source of mineralizing fluid proposed earlier. Geological and petrological data indicate autometasomatic alteration of alkaline granites (BOWDEN, 1982; KINNAIRD, 1985). Oxygen isotope data point to fluid-granite interaction during the Nigerian emerald growth (GIULIANI et al., 1998). Studied oversaturated brine inclusions are also characteristic for silicic magmas (BODNAR, 1994), greisen and skarns associated with granite domes (KWAK, 1987). The obtained relatively low pressure (depth) and high temperature of the emerald growth indicate the very high geothermal gradient during the emerald formation. It seems reasonable to connect the high geothermal gradient with the intrusion of granite.

Conclusion

The fluid inclusions in the emerald associated with the Younger Granites of Central Nigeria (the

Jos complex) were investigated. Fluid inclusions of primary and pseudosecondary origin unambiguously characterize the composition of the fluid phase participating in the emerald growth. It was a Na–Ca–Cl solution with a $NaCl/CaCl_2$ ratio of about 3:1, a total bulk salinity of about 40–45 wt%, and with a few wt% of volatiles ($CO_2 \pm CH_4 \pm H_2S$). CO_2 is of low density (up to 0.13 g/cm^3), liquid CO_2 is not visible at room temperature. The daughter phases are represented by halite, calcite, Mg-calcite and aragonite.

Th of fluid inclusions is about 400–450 °C. The trapping conditions of fluid inclusions within the early and intermediate growth zones of the emerald were determined as: T ≈ 400–450 °C, P ≈ 0.2–0.3 kbar.

Many characteristics of fluid inclusions in the Nigerian and Colombian emeralds are similar. Nevertheless, a number of criterion on fluid inclusions permits easily to distinguish the Nigerian and Colombian emeralds.

Acknowledgements

We are very much obliged to O. Navon (The Hebrew University of Jerusalem) for his kind permission to use the Raman microprobe for the inclusion study of emeralds. We are thankful to G. Giuliani and J. Mullis for their profound and constructive review of our paper.

References

BANKS, D.A., YARDLEY, B.W.D., GIULIANI, G., CHEILLETZ, A. and RUEDA, F. (1995): Chemistry and source of the high-temperature brines in the Colombian emerald deposits. In: PASAVA, J., KRIBEK, B. and ZAK, K. (eds): Mineral deposits: From their origin to their environmental impacts, Prague, August 28–31, SGA Meeting on Mineral Deposits, 557–560.

BEUS, A.A. and DIKOV, YU.P. (1967): Geochemistry of beryllium in the processes of endogenic mineral-formation, Nedra, Moscow (in Russian).

BEUS, A.A. and MINEYEV, D.A. (1974): Contribution to geology and geochemistry of the emerald-bearing zone Muzo-Coscuez, Cordillera Oriental, Colombia. Geol. Rundsch. Mestorozhd. 16, 18–30 (in Russian).

BODNAR, R.J. (1994): Philosophy of fluid inclusion analysis. In: DE VIVO, B. and FREZZOTTI, M.L. (eds): Fluid inclusions in minerals: Methods and applications, Virginia Tech. 1–6.

BODNAR, R.J. and VITYK, M.O. (1994): Interpretation of microthermometric data for H_2O–NaCl fluid inclusions. In: DE VIVO, B. and FREZZOTTI, M.L. (eds): Fluid inclusions in minerals: Methods and applications, Virginia Tech. 117–130.

BOWDEN, P. (1982): Magmatic evolution and mineralization in the Nigerian Younger Granite province. In: EVANS, A.M. (ed.): Metallisation Associated with Acid Magmatism, John Wiley, London.

BROWN, G. and DIP, D.T. (1984): Australia's first emeralds. J. Gemm. 19, 320–335.

BROWN, P.E. and LAMB, W.M. (1989): P–V–T properties of fluids in the system $H_2O \pm CO_2 \pm$ NaCl. New graphical presentations and implications for fluid inclusion studies. Geochim. Cosmochim. Acta 53, 1209–1221.

BROWN, P.L., ELLIS, J. and SYLVA, R.N. (1983): The hydrolysis of metal ions. 7. Beryllium (II). J. Chem. Soc., Dalton Trans., 2001–2004.

BURKE, E.A.J. (1994): Raman microspectrometry of fluid inclusions: The daily practice. In: DE VIVO, B. and FREZZOTTI, M.L. (eds): Fluid inclusions in minerals: Methods and applications, Virginia Tech. 25–44.

CHEILLETZ, A., FÉRAUD, G., GIULIANI, G. and RODRIGUEZ, C.T. (1994): Time-pressure and temperature constraints on the formation of Colombian emeralds: An $^{40}Ar/^{39}Ar$ laser microprobe and fluid inclusion study. Econ. Geol. 89, 361–380.

CHEILLETZ, A. and GIULIANI, G. (1996): The genesis of Colombian emeralds: a restatement. Mineral. Deposita 31, 359–364.

DICKIN, A.P., HALLIDAY, A.N. and BOWDEN, P. (1991): A Pb, Sr and Nd isotope study of the basement and Mesozoic ring complexes of the Jos Plateau, Nigeria. Chem. Geol. 94, 23–32.

GIARD, D., GIULIANI, G., CHEILLETZ, A., FRITSCH, E. and GONTHIER, E. (1998): L'émeraude. Connaissances actuelles et prospectives. AFG, CNRS, ORSTOM (eds), Paris, 233 pp.

GIULIANI, G., SHEPPARD, S.M.F., CHEILLETZ, A. and RODRIGUEZ, C. (1992): Contribution de l'etude des phases fluides et de la géochimie isotopique $^{18}O/^{16}O$, $^{13}C/^{12}C$ à la genèse des gisements d'émeraude de la Cordillère orientale de la Colombie. C. R. Acad. Sci. Paris 314, 269–274.

GIULIANI, G., CHEILLETZ, A., DUBESSY, J. and RODRIGUEZ, C.T. (1993): Chemical composition of fluid inclusions in Colombian emerald deposits. Proc. Eighth Quadrennial IAGOD Symposium, 159–168.

GIULIANI, G., CHEILLETZ, A., ARBOLEDA, C., CARILLO, V., RUEDA, F. and BAKER, H. (1995): An evaporitic origin of the parent brines of Colombian emeralds: Fluid inclusion and sulfur isotope evidence. Europ. J. Mineral. 7, 151–165.

GIULIANI, G., CHEILLETZ, A., ZIMMERMANN, J.-L., RIBEIRO-ALTHOFF, A.M., FRANCE-LANORD, C. and FERAUD, G. (1997): Les gisements d'émeraude du Brésil: genèse et typologie. Chronique de la Recherche Minière 526, 17–61.

GIULIANI, G., FRANCE-LANORD, C., COGET, P., SCHWARZ, D., CHEILLETZ, A., BRANQUET, Y., GIARD, D., MARTIN-IZARD, A., ALEXANDROV, P. and PIAT, D.H. (1998): Oxygen isotope systematics of emerald: relevance of its origin and geological significance. Mineral. Deposita 31, 513–519.

GOVOROV, I.N. and STUNZHAS, A.A. (1963): Mode of transport of beryllium in alkali metasomatism. Geochem. Int. 4, 402–409.

GRAZIANI, G., GÜBELIN, E. and LUCCHESI, S. (1983): The genesis of an emerald from the Kitwe District, Zambia. N. Jb. Miner. Mh. 4, 175–186.

GRUNDMANN, G. and MORTEANI, G. (1989): Emerald mineralization during regional metamorphism: Habachtal (Austria) and Leydsdorp (Transvaal, South Africa) deposits. Econ. Geol. 84, 1835–1849.

HAYNES, F.M. (1985): Determination of fluid inclusion compositions by sequential freezing. Econ. Geol. 80, 1436–1439.

KAZMI, A.H. and SNEE, L.W. (1989): Emeralds of Pakistan: geology, gemology and genesis. In: KAZMI, A.H. and SNEE, L.W. (eds): Van Nostrand Reinhold publishers, 269 pp.

KINNAIRD, J.A. (1979): Mineralisation associated with The Nigerian Mesozoic ring complexes. Stud. Geol. Salamanca. 14, 189–220.

KINNAIRD, J.A. (1985): Hydrothermal alteration and mineralization of the alkaline anorogenic ring complexes of Nigeria. J. African Earth Sci. 3, 229–251.

KIYEVLENKO, YE.YA., SENKEVICH, N.N. and GAVRILOV, A.P. (1974): Geology of gemstone deposits, Nedra, Moscow, 345 pp. (in Russian).

KWAK, T.A.P. (1987): W–Sn skarn deposits and related metasomatic skarns and granitoids. Developments in Economic Geology, Elsever Science Publishers B. V., 24, 451 pp.

LAURS, B.M., DILLES, J.H. and SNEE, L.W. (1996): Emerald mineralization and metasomatism of amphibolite, Khaltaro garanitic pegmatite hydrothermal vein system, Haramosh mountains, northern Pakistan. Can. Mineral. 34, 1253–1286.

MOROZ, I.I. (1978): Principal features of geochemistry of emerald-bearing micaceous metasomatites from the Urals. Bull. High Education Institutions, Geol. Prospecting, 1151, 1–28 (in Russian).

MOROZ, I.I. (1979): The mineralogy of primary aureoles of emerald-bearing micaceous rocks. Miner. Mag. Lvov St. Univ., 33, 116–120 (in Russian).

MOROZ, I.I. (1983): Forms of occurrence of element-indicators in the primary haloes of emerald-bearing phlogopites in an Uralian deposit. International Geol. Rev. 25, 1021–1026.

MOROZ, I.I. (1996): Geochemistry of the emerald-bearing micaceous rocks from the Urals. Abst. Isr. Geol. Soc. Annu. Meeting, p. 71.

MOROZ, I.I. and ELIEZRI, I.Z. (1998a): Emerald chemistry from different deposits: an electron microprobe study. Australian Gemm. 20, 64–69.

MOROZ, I.I. and ELIEZRI, I.Z. (1998b): Phyllosilicate inclusions in emeralds from various deposits. IMA Meeting Abstracts with Programs 1998, Toronto, Canada, p. 16.

MOROZ, I. and VAPNIK, YE. (1998): Fluid inclusions in emeralds from various deposits. GSA Meeting Abstracts with Programs 1998, Toronto, Canada, p. A–382.

MOROZ, I.I. and ELIEZRI, I.Z. (1999): Mineral inclusions in emeralds from different sources. J. Gemm. 6, 357–363.

MOROZ, I. and VAPNIK, YE . (1999): Fluid inclusions in emeralds from schist-type deposits. Canadian Gemm. XX, 8–14.

NWE, Y.Y. and MORTEANI, G. (1993): Fluid evolution in the H_2O–CH_4–CO_2–NaCl system during emerald mineralization at Gravelotte, Murchison Greenstone Belt, Northeast Transvaal, South Africa. Geochim. Cosmochim. Acta 57, 89–103.

ROEDDER, E. (1984): Fluid inclusions. Reviews in mineralogy, Vol. 12. Mineralogical Society of America, Washington, DC, 644 pp.

RUDOWSKI, L. (1989): Pétrologie et géochimie des granites transamazoniens de Campo Formoso et Carnaiba (Bahia, Brésil) et des phlogopitites à émeraude associées. Thèse Doctorat, Université Paris VI, 291 pp.

SCHWARZ, D. (1987): Esmeraldas – Inclusões en gemas. Imprensa Universitária UFOP, Ouro Preto, 450 pp.

SCHWARZ, D. (1991): Australian emeralds. Australian Gemm. 488–497.

SCHWARZ, D. and EIDT, T. (1989): The Brazilian emeralds and their occurrences: Carnaiba, Bahia. J. Gemm. 21, 474–486.

SCHWARZ, D., KANIS, J.and KINNAIRD, J. (1996): Emerald and green beryl from Central Nigeria. J. Gemm. 25, 117–141.

SHMULOVICH, K.I., TERESHENKO, YE.N. and KALINICHEV, A.G. (1982): Equation of state and isochores of nonpolar gases up to 2000 K and 10 GPA. Geochimiya, 11, 1598–1614 (in Russian).

SINKANKAS, J. and READ, P. (1986): Beryl. Butterworths Gem Books, 255 p.

SLIWA, A.S. and NGULUWE, C.A. (1984): Geological setting of Zambian emerald deposits. Precambrian Res. 25, 213–228.

SOUZA, J.L., MENDES, J.C., DA SILVEIRA BELLO, R.M., SVISERO, D.P. and VALARELLI, J.V. (1992): Petrographic and microthermometrical studies of emeralds in the "Garimpo" of Capoeirana, Nova Era, Minas Gerais State, Brazil. Mineral. Deposita, 27, 161–168.

VANKO, D.A., BODNAR, R.J. and STERNER, S.M. (1988): Synthetic fluid inclusions: VIII. Vapor-saturated halite solubility in part of the system NaCl–$CaCl_2$–H_2O, with application to fluid inclusions from oceanic hydrothermal systems. Geochim. Cosmochim. Acta 52, 2451–2456.

VITYK, M.O. and BODNAR, R.J. (1998): Statistical microthermometry of synthetic fluid inclusions in quartz during decompression reequilibration. Contrib. Mineral. Petrol. 132, 149–162.

WOOD, S.A. (1992): Theoretical prediction of speciation and solubility of beryllium in hydrothermal solution to 300 °C and saturated vapor pressure: application to bertrandite/phenacite deposits. Ore Geol. Rev. 7, 249–278.

ZWART, E.W. and TOURET, J.L.R. (1994): Melting behavior and composition of aqueous fluid inclusions in fluorite and calcite: applications within the system H_2O–$CaCl_2$–NaCl. Eur. J. Mineral. 6, 773–786.

Manuscript received May 10, 1999; revision accepted March 6, 2000.